EFFECTS OF HOMOGENEOUS AND HETEROGENEOUS REACTIONS ON THE WATER-BASED NANOFLUID STREAMING ABOVE AN EXTENDING SURFACE

D. DEY, R. BORAH and M. HAZARIKA

Department of Mathematics, Dibrugarh University, Dibrugarh-786004, Assam
Emails: debasish41092@gmail.com, rpjtbrh@gmail.com, madhuryahazarika1995@gmail.com

***Abstract*—The effect of homogeneous and heterogeneous reactions, as well as second-order velocity slip, on the magnetic influenced flow of nanofluid (Cu-water and MgO-water) passing above an extending surface has been examined. To alter the nature of the leading equations of this problem, a new set of dimensionless variables have been employed. The resulting equations with the corresponding surface restrictions are solved using the Runge-Kutta-Fehlberg technique (RKF45) by developing a code in Maple-18. The outcomes of this investigation are presented in terms of pictorial mode with the effects of different novel flow parameters. Also, numerical values of physical quantities that are associated with this problem are set in terms of tabular mode. It is perceived that with increasing the number of solid particles, the thermal and mass fractions of the nanofluid behave as an enhancing function, whereas the motion of the nanofluid is a decreasing function.**

Keywords*—Nanofluid, heat transfer, MHD, homogeneous and heterogeneous reaction, velocity slip, Runge-Kutta-Fehlberg technique

I. INTRODUCTION

The fluid streaming above an elongating surface has multifarious applications in engineering sciences, medical sciences and industrial problems. The fluid flow along with thermal and mass transmissions over an elongating type geometry have different applications. Polymer extrusion, wire drawing, paper production and annealing and thickening of copper wire are some important applications of this type of surface. Crane (1970) was the first author who formulated a mathematical model of viscous fluid flow caused due to an extending surface. In the recent time, many authors such as Muhammad *et al.* (2019), Khashi'ie *et al.* (2019), Dey and Borah (2020, 2021), Dey *et al.* (2021a) and Dey *et al.* (2021b) have explored their ideas of the border-layer flow of different fluid models by considering the present geometries. Recently, Dey *et al.* (2022) and Jeevandhar *et al.* (2021) have investigated the boundary layer flow with the effects of the magnetic field by taking elongating geometries under the different fluid models. The fluid flow containing nanoparticles over an extending/contracting geometry has important in modern technology.

Enhancement of heat transfer rate or energy transfer is the key requirement of all modern industries. Numerous unique methods have been employed for several decades to develop heat transfer rates and achieved different levels of thermal efficiencies. Scientists and researchers have developed a technique to control the heat transfer rate by adding nanoparticles of sized 1-100 nm in a traditional fluid. This development has taken a great deal of interest in modern times due to its imperative applications in different physical fields. The nanoparticles utilized in nanofluids are naturally prepared of metals, oxides, carbides or nitrides etc and the traditional fluid is regularly a heat transfer fluid like water (as in this study), kerosene and different bio-fluids etc. Choi (1995) was the first author who proposed the term 'nanofluid' experimentally. These smart fluids have numerous applications in engineering sciences, bio-medical sciences and industrial processes etc. This special type of fluid is responsible for the enhancement of the thermal conductivity of the fluid. Anuar *et al.* (2019) have investigated the thermally stratified nanofluid flow containing *CuO* & *Ag* by considering an exponential form of contracting surface. Alzahrani *et al.* (2021) have investigated the importance of solar energy by considering nanofluids containing different nanoparticles such as *CuO* & *MgO*etc. Recently, many researchers Shravani *et al.* (2018), Rajesh *et al.* (2020), Dey and Chutia (2020), Zehra *et al.* (2021), Ho *et al.* (2021), Prasannakumara (2021), Jamshed *et al.* (2021) and Dey and Hazarika (2021), etc.; have investigated the nature of nanofluids flow caused due to different geometries with thermal transmission by considering different base fluids. Mehdi *et al.* (2022) have investigated the heat transfer phenomena in presence of the magnetic field of the nanofluid flow between two parallel disks of infinite lengths. Recently, Hasnain and Abbas (2019), Abbas *et al.* (2021), Naveed *et al.* (2021), Hasnain and Abid (2022) and Hasnain *et al.* (2021) have analyzed the nanofluids flow under the different novel flow factors by taking different geometries and methods.

The movement of boundary layer fluids associated with a magnetic field is becoming increasingly important in various industrial concerns as well as in describing the behavior of the sun and stars. We can readily describe the formation of the solar halo via magneto-hydrodynamic (MHD) theory. Since magneto-hydrodynamic can gyrate the magnetic field and the affecting fluid generates electricity. MHD has a variety of uses, including blood plasma and blood pump equipment. Chemical reactions in conjunction with magnetic fields have once again piqued people's interest in current times. Chemical reactions in the current fluid model occur in a variety of chemically reactive systems, including incineration, catalysis, and biochemical systems. The harmonized reactions generally happen in the whole fluid bulk in the same phase and the assorted reactions happen on some catalytic surfaces in two or more phases. In 1996, Markin (1996) formulated a mathematical model for isothermal homogeneous-heterogeneous chemical reactions in boundary-layer fluid flow caused due to a vertical plate. Recently, Sheikh and Abbas (2017) have formulated a model of the present considering chemical reactions in a viscous fluid flow by considering the Casson fluid model. Hayat *et al.* (2017) have analyzed the importance of the present considering chemical reactions in the magnetized border-layer flow of water-based nanofluid containing *Cu* & *Ag* by considering first-order velocity slip. Almutairi *et al.* (2019) have extended this work by adopting the model of this problem. Malik and Khan (2018) have analyzed the effects of both chemical reactions numerically. Doh *et al.* (2020) have analyzed the consequences of both harmonized and assorted chemical reactions on the nanofluid flow due to a rotating disc. Waini *et al.* (2021) have studied the importance of chemical reactions in the form of the present model by adopting a hybrid nanofluid flow caused due to a shrinking/stretching surface. Sheikh *et al.* (2021) have analyzed the boundary-layer flow due to an extending plate with the influence of heat transfer phenomena in presence of both homogeneous and heterogeneous chemical reactions.

The main intention of this present problem is to explore the persuade of the present considering chemical reactions on the thermally stratified water-based nanofluid containing the nanoparticles *Cu* & *MgO* streaming above an extending surface with a second-order velocity slip. The leading equations of this problem are developed by using some physical assumptions and laws. For solving these supported equations, a special set of new variables is introduced that gives a set of a solvable form of equations. This set of equations is decoded utilizing the Runge-Kutta-Fehlberg technique (RKF45) by developing the code of a symbolic computer algebra program in Maple 18. The outcomes of this study have been established in terms of both pictorial and tabular forms with significant values of flow parameters. To give conformity to our numerical codes, we have compared our numerical values with the results reported in Hayat *et al.* (2017) and Almutairi *et al.* (2019). Hayat *et al.* (2017) have explored the flow behaviour of the nanofluid in the presence of both homogeneous and heterogeneous chemical reactions with first-order velocity slip conditions. Almutairi *et al.* (2019) have extended this work by considering second-order velocity slip conditions using the Homotopy Analysis method. To the best of the authors' knowledge, analysis of the MHD boundary-layer flow of

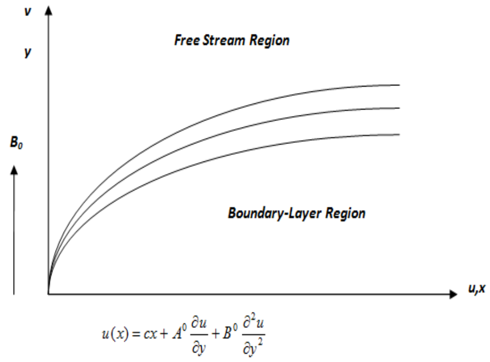

Figure 1. Schematic diagram of the present model.

water-based nanofluid due to an extending surface and thermal transference in presence of homogeneous-heterogeneous chemical reactions with second-order boundary slip conditions have not been considered so far. Here, we have taken the nanoparticles Copper (*Cu*) and Magnesium Oxide (*MgO*) to form water-based nanofluids. These nanoparticles have multifarious applications in different industrial processes and played an important role to enhance thermal transmission.

II. MATHEMATICAL FORMULATION

We consider the time-independent, incompressible and two-dimensional boundary-layer flow of water-based nanofluid containing the nanoparticles Cu and MgO which is positioned in an extending porous medium. A homogeneous magnetic field of potency B_0 is concerned in the normal direction of the flow. The sheet is characterized by the velocity $u(x) = cx + U_{slip}$, where $c > 0$ recognizes the stretch at the surface and U_{slip} the velocity slip and the prescribed wall temperature is $T = T_w$. The flow diagram of this problem is shown in Fig. 1.

A simple homogenous-heterogeneous reaction model with chemical orders A and B is adopted by motivating Hayat *et al.* (2017) and Almutairi *et al.* (2019) which is explained in the following way. For cubic auto-catalysis, the homogenous reaction is exemplified by Eq. (1) and an isothermal reaction of first-order (heterogeneous reaction) on the catalyst surface is represented as Eq. (2).

$$A + 2B \rightarrow 3B, \text{rate} = K_c a b^2 \quad (1)$$

$$A \rightarrow B, \text{rate} = K_s a \quad (2)$$

In this study, we have assumed that both reaction processes are isothermal. By employing the above suppositions, the supported leading equations of this problem are illustrated in the following way (Hayat *et al.*, 2017; and Dey and Hazarika, 2022):

$$\frac{\partial u}{\partial x} + \frac{\partial v}{\partial y} = 0, \quad (3)$$

$$\rho_{nf}\left(\frac{\partial u}{\partial x} + v\frac{\partial u}{\partial y}\right) = \mu_{nf}\frac{\partial^2 u}{\partial y^2} - \mu_{nf}\frac{1}{K}u - \sigma_{nf}B_0^2 u, \quad (4)$$

$$\rho_{nf}\left(u\frac{\partial T}{\partial x} + v\frac{\partial T}{\partial y}\right) = \frac{k_{nf}}{(\rho C_p)_{nf}}\frac{\partial^2 T}{\partial y^2} - \frac{\mu_{nf}}{(\rho C_p)_{nf}}\frac{\partial u}{\partial y} - \frac{\sigma_{nf}}{(\rho C_p)_{nf}}B_0^2 u^2, \quad (5)$$

$$u\frac{\partial a}{\partial x} + v\frac{\partial a}{\partial y} = D_A\frac{\partial^2 a}{\partial y^2} - K_c a b^2, \quad (6)$$

$$u\frac{\partial b}{\partial x} + v\frac{\partial b}{\partial y} = D_B\frac{\partial^2 b}{\partial y^2} - K_c a b^2, \quad (7)$$

Equations (3)-(5) are derived from the principle of conservation of mass, linear momentum and energy respectively under the above considering assumptions. The equation of motion (Eq. 4) is governed by the inertia force (left-hand side), viscous force (1st term of right-hand side), Darcy's force (2nd term of right-hand side) and Lorentz force (last term of right-hand side). In the equation of energy (Eq. 5), flow is maintained with free convection (left-hand side) and conduction (1st term of the right-hand side) heat transfers. The 2nd and 3rd terms of right hand side of Eq. (5) represent the effects of energy dissipation and Ohmic heating respectively. Equations (6) and (7) are derived from the principle of conservation of species and the flow is maintained with convection and diffusion mass transfers under the influence of homogeneous and heterogeneous chemical reactions.

The restrictions at the surface and free stream region are

$$y = 0: u = cx + U_{slip}, v = 0, T = T_w, \quad (8)$$
$$D_A \frac{\partial a}{\partial y} = K_s a,\ D_B \frac{\partial b}{\partial y} = -K_s a,$$
$$y \to \infty: y \to 0, T \to T_\infty, a \to a_0, b \to 0. \quad (9)$$

where, U_{slip} is the second-order slip velocity at the sheet and is defined as given below (referring Fang *et al.*, 2010; Fang and Aziz, 2010 and Almutairi *et al.*, 2019):

$$U_{slip} = \frac{2}{3}\left(\frac{3-\varepsilon l_1^2}{\varepsilon} - \frac{3}{2}\frac{1-l_1^2}{K_n}\right)\delta_1 \frac{\partial u}{\partial y} - \frac{1}{4}\left[l_1^4 + \frac{2}{K_n^2}(1-l_1^2)\right]\delta_1^2 \frac{\partial^2 u}{\partial y^2},$$
$$U_{slip} = A^0 \frac{\partial u}{\partial y} + B^0 \frac{\partial^2 u}{\partial y^2} \quad (10)$$

where, A^0 and B^0 are constants, K_n the Knudsen number that quantifies the molecular mean free path such that velocity slip reduces with smaller values of K_n and $0 \le l_1 = \min\left(\frac{1}{K_n}, 1\right) \le 1$. Here, the constant $B^0 < 0$ because δ_1 is always positive.

The relationship of the thermo-physical properties between base fluid and nanofluid are defined in the following way (Mishra *et al.*, 2019; Dey and Hazarika, 2022; and Hasnain *et al.*, 2022):

$$\rho_{nf} = \rho_f(1-\phi) + \rho_S\phi, \mu_{nf} = \mu_f(1-\phi)^{-2.5},$$
$$(\rho C_p)_{nf} = (\rho C_p)_f(1-\phi) + (\rho C_p)_S\phi,$$
$$k_{nf} = k_f\left[\frac{k_S^* + 2k_f - 2\phi(k_f - k_S^*)}{k_S^* + 2k_f + 2\phi(k_f - k_S^*)}\right] \quad (11)$$
$$\sigma_{nf} = \sigma_f\left[1 + \frac{3(\sigma-1)\phi}{2+\sigma-(\sigma-1)\phi}\right], \sigma = \frac{\sigma_s}{\sigma_f}.$$

To alternate the nature of non-linear supported Eqs. (3)-(7) along with boundary condition (8), a mass preservation similarity transformation is employed which is defined as the Eq. (12).

$$\eta = \sqrt{\frac{c}{\upsilon_f}}y, u = cxf'(\eta), v = -\sqrt{c\upsilon_f}f(\eta), \quad (12)$$
$$a = a_0 g(\eta), b = a_0 h(\eta), \theta(\eta) = \frac{T-T_\infty}{T_w - T_\infty}.$$

Equation (12) modernizes the supported equations into a set of coupled non-linear ordinary differential equations which is solvable. We have achieved the following solvable equations and the related surface restriction:

$$\beta_1 f'''(\eta) - \beta_1\lambda f'(\eta) - \beta_2 M f'(\eta) + f'(\eta)f''(\eta) - f''(\eta) = 0, \quad (13)$$
$$\beta_3\theta''(\eta) + \beta_4 \Pr Ec\, f''(\eta)^2 + \beta_5 \Pr MEc\, f'(\eta)^2 + \Pr f(\eta)\,\theta'(\eta) = 0, \quad (14)$$
$$g''(\eta) + Scf(\eta)g'(\eta) - Sckg(\eta)h^2(\eta) = 0, \quad (15)$$
$$\delta h''(\eta) + Scf(\eta)h'(\eta) + Sckg(\eta)h^2(\eta) = 0. \quad (16)$$

where the constants are defined in the following way:

$$\beta_1 = \frac{\mu_{nf}\rho_f}{\mu_f\rho_{nf}}, \beta_2 = \frac{\sigma_{nf}\rho_f}{\sigma_f\rho_{nf}}, \beta_3 = \frac{k_{nf}(\rho C_p)_f}{k_f(\rho C_p)_{nf}},$$
$$\beta_4 = \frac{\mu_{nf}(\rho C_p)_f}{\mu_f(\rho C_p)_{nf}} \text{ and } \beta_4 = \frac{\sigma_{nf}(\rho C_p)_f}{\sigma_f(\rho C_p)_{nf}}.$$

The dimensionless flow parameters are defined below:

$$\lambda = \frac{\upsilon_f}{cK}, M = \frac{\sigma_f B_0^2}{\rho_f c}, \Pr = \frac{\upsilon_f}{\alpha_f}, Ec = \frac{u_W^2}{(C_p)_f(T_W - T_\infty)},$$
$$Sc = \frac{\upsilon_f}{D_A}, k = \frac{K_c a_0^2}{c}, \delta = \frac{D_A}{D_B}, k_s = \frac{K_S}{D_A}\sqrt{\frac{\upsilon_f}{c}},$$
$$\gamma_1 = A^0\sqrt{\frac{c}{\upsilon_f}} \text{ and } \gamma_2 = B^0\frac{c}{\upsilon_f}.$$

The restrictions at the surface and free stream region are:

$$f'(0) = 1 + \gamma_1 f''(0) + \gamma_2 f'''(0), f(0) = 0,$$
$$\theta(0) = 1, g'(0) = K_s g(0), \delta h'(0) = -K_s g(0), \quad (17)$$
$$f'(\infty) \to 0, \theta(\infty) \to 0, g(\infty) \to 1, h(\infty) \to 0.$$

where $\gamma_1 > 0$ and $\gamma_2 < 0$ are the velocity slip parameters. The diffusion coefficients of D_A and D_B are accepted to be of an equivalent form i.e., $\delta = 1$.

In this situation, we have from Eq. (17), $g(\eta) + h(\eta) = 1 \Rightarrow h(\eta) = 1 - g(\eta)$, then combining the Eqs. (15) and (16) which are associated with the surface conditions and Eqs. (15) and (16) become:

$$g''(\eta) + Scf(\eta)g'(\eta) - Sckg(\eta)[1-g(\eta)]^2 = 0, \quad (18)$$
$$g'(0) = K_s g(0), g(\infty) \to 1. \quad (19)$$

III. PHYSICAL QUANTITIES

In this analysis, three physical numbers such as drag force, rate of heat transfer and mass accumulation rate of the fluid at the surface are observed. These numbers are the most important quantities in different physical fields such as engineering sciences, aircraft, geo-physics etc. These quantities are discussed in terms of C_f, Nu_f and Sh_x and defined in the following way:

$$C_f = -\frac{\mu_{nf}}{0.5\rho_f u_W^2}\frac{\partial u}{\partial y}\bigg|_{y=0}, Nu_x = -\frac{k_{nf}}{k_f}\frac{x}{(T_W - T_\infty)}\frac{\partial T}{\partial y}\bigg|_{y=0}. \quad (20)$$

Using the Eq. (12), we have achieved the expression of the dimensionless physical quantities as:

$$C_f\sqrt{\mathrm{Re}_x} = -\frac{1}{(1-\phi)^{2.5}}f''(0),$$
$$Nu_x \mathrm{Re}_x^{-1/2} = \frac{k_{nf}}{k_f}\theta'(0). \quad (21)$$

where $\mathrm{Re}_x = u_w x/\upsilon_f$.

Table 1. Thermo-physical properties of water-based nanoparticles (referring Hussain *et al.*, 2014; Chanie *et al.*, 2018; Khashi´ie *et al.*, 2019; Alzahrani *et al.*, 2021; and Ismail *et al.*, 2018).

Physical Properties	Water	*MgO*	*Cu*
$\rho(Kgm^{-3})$	997.1	3580	8933
$C_p(J(Kg.K)^{-1})$	4179	960	385
$K(W(M.K)^{-1})$	0.6130	48.4	401
$\sigma(sm^{-1})$	5.5×10^{-6}	1.42×10^{-3}	59.6×10^{6}

IV. METHODOLOGY

Due to the presence of non-linearity in the resultant equations, the analytical approach for solving this type of equation is not fit suitably. So, we have employed the RKF45 (Runge-Kutta-Fehlberg fourth-fifth order) method with the help of symbolic algebra software Maple-18 (referring Bachok *et al.*, 2013; and Rahman and Eltayeb, 2013) for solving Eqs. (13, 14) and (18) along with the surface restrictions (17) and (19). Maple is math software that merges the world's most powerful math engine with an interface that makes it extremely easy to analyze, explore, visualize and solve mathematical problems. RKF45 is based on a numerical algorithm that is very competent to work out this type of problem. It controls the error automatically using rules 4 and 5. In this problem, it is observed that the solution converged when $\eta \to 7$ and $\eta \to 10$, hence ∞ is replaced by 7 and 10 throughout the investigation. The procedure of RKF45 code in Maple software is briefly discussed by Aziz (2009).

V. RESULTS AND DISCUSSIONS

Mathematical results for different novel physical parameter values are acquired to realize an understanding of the physical problem. Numerical results for different flow parameters such as M, ϕ, λ_1, λ_2, Pr and k_s are achieved and these outcomes are discussed explicitly in terms of graphs and tabular forms. We have taken $M = 0.5$, $\phi = 0.2$, $\lambda_1 = 0.4$, $\lambda_2 = -0.60$, $\Pr = 6.2$, $Sc = 0.60$, $k_s = k = 0.3$ and $\lambda = 0.4$ constant throughout the investigation unless otherwise mentioned except for the concerned parameter under analysis. In this study, we have taken the nanoparticles *Cu* & *MgO* with the base fluid water. For clear understanding, solutions of *Cu* & *MgO* nanoparticles are denoted as dashed lines and solid lines respectively.

Figures (2)-(4) are designed to show the action of M on the velocity pattern, temperature distributions and mass fraction of the nanofluid respectively. Due to the application of a transverse magnetic field on the nanofluid, a force is developed called 'Lorentz force'. This developing force has the propensity to enhance the resistance force which reduces the speed of the nanofluid. Hence the motion slows down with the rise of the magnetic parameter (Fig. 2). From Fig. (2), it is also perceived that the velocity of the *MgO* nanofluid is comparatively higher than *Cu* nanofluid. Again, due to the slowdown of the fluid motion, one kind of heat develops that rises the temperature distributions of the nanofluid, as demonstrated in Fig. 3. The thermal boundary layer thickness of the water-based fluid containing *MgO* is smaller than the *Cu* -nanofluid. From Fig. (4), it is detected that the improving values of M enhances the mass fraction of the nanofluid. Also, the concentration borderline width of the *MgO* -nanofluid is larger than *Cu*

The influence of ϕ (volume fraction of nanoparticles) is discussed in Figs. (5)-(7). Figure (5) demonstrates that with the increase of volume fraction, there is deceleration in fluid motion during *Cu*-water and *MgO* -water cases. This is because the Lorentz force persuades the accumulation of more conducting nanoparticles into the liquids and hence the velocity pattern drops down. Again, velocity of "*MgO* -water" nanofluid is higher than "*Cu* -water"

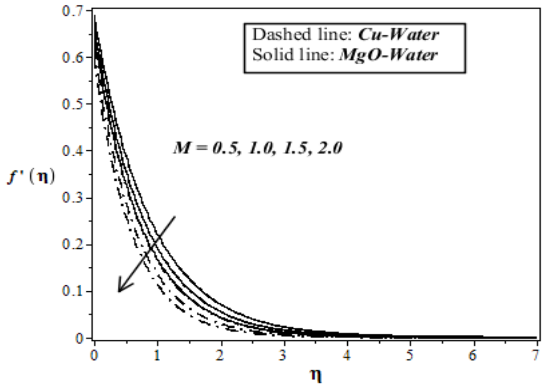

Figure 2. Action of M on the velocity pattern.

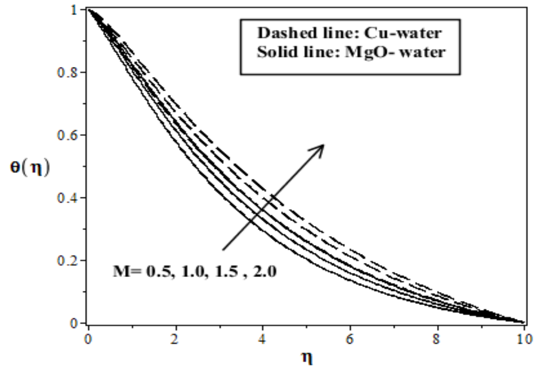

Figure 3. Action of M on the temperature distributions.

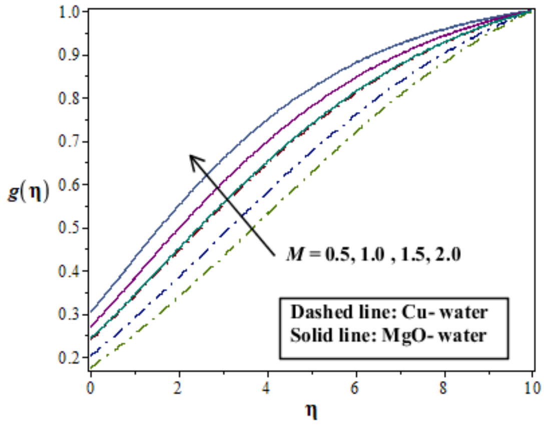

Figure 4. Action of M on the mass fraction of the fluid.

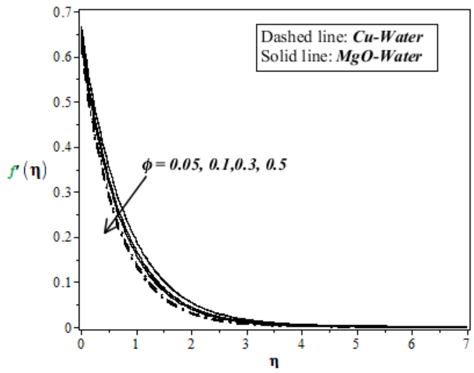

Figure 5. Action of ϕ on the velocity pattern.

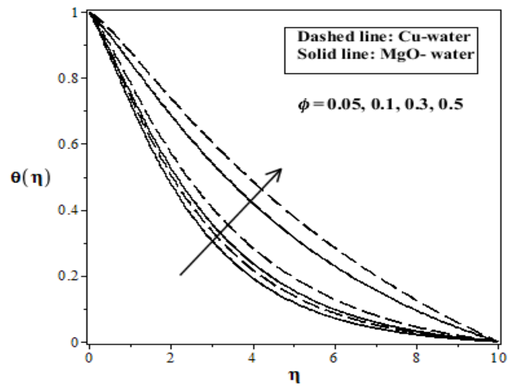

Figure 6. Action of ϕ on the temperature distributions.

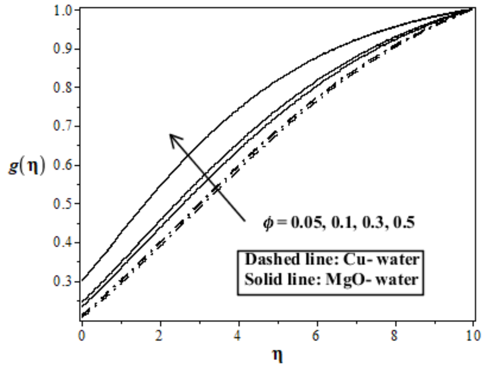

Figure 7. Action of ϕ on the mass fraction of the fluid.

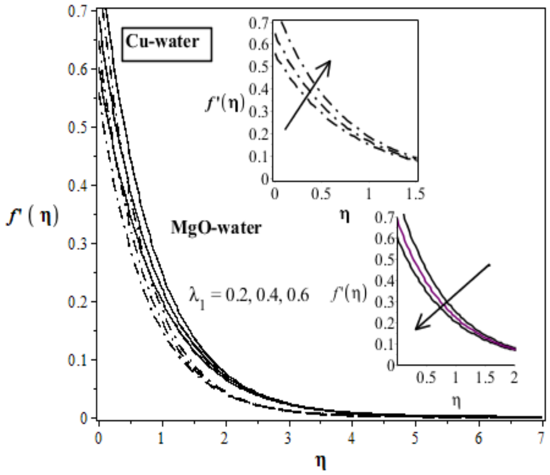

Figure 8. Action of λ_1 on the velocity pattern.

nanofluid. Figure (6) illustrates the temperature distributions for improving values of ϕ The nanoparticles physically disperse energy in terms of heat. Due to this physical phenomenon, the temperature distributions of the "*MgO* -water" based nanofluid higher than "*Cu* -water" based nanofluid. Figure (7) is depicted to show the action of volume fraction on the mass fraction of the fluid. It is perceived that the mass fraction for both the liquids boosts up with ϕ Again, the concentration boundary-layer thickness for the *MgO* -nanofluid is larger than *Cu*.

Action of 1st and 2nd order velocity slip parameters (λ_1 and λ_2) on the velocity distribution, temperature and concentration pattern of the nanofluid are discussed in Figs. (8)-(10). Figure (8) illustrates the motion of the nanofluid containing the nanoparticles *Cu* and *MgO* with the effects of λ_1 The *MgO* -nanofluid velocity enhances with λ_1 (Fig. 8). But an opposite nature is developed for the *Cu*-nanofluid. Figure (9) represents the mass fraction of the nanofluid with the 1st order velocity slip parameter. The first-order velocity slip parameter lessens the mass fraction of the nanofluid and the concentration boundary-layer thickness of the "*MgO* -water" nanofluid is higher in comparison to the "*Cu* -water" nanofluid. Figure (10) depicts the influences of λ_2 on the velocity, temperature and mass fraction of the nanofluids. The momentum boundary-layer thickness for the *Cu*-nanofluid is smaller than *MgO* -water based nanofluid under the influence of the second-order velocity slip parameter. Again, the thermal boundary-layer thickness for *MgO* -water nanofluid is lesser than *Cu*-water nanofluid under the influence of λ_2. The mass fraction of the nanofluid containing *MgO* nanoparticle is higher than *Cu*-nanoparticle. Figure (11) is depicted to illustrate the influence of the Prandtl number on the temperature distribution of the nanofluid. It is noticed that the thermal transmission of the nanofluid has been reduced with the improving values of Pr. It is also perceived that the temperature of the *Cu*-H_2O nanofluid is larger in comparison to *MgO*-H_2O nanofluid during the effects of Pr. In general, when $\Pr = 1$, it means that the influence of the momentum and thermal diffusions is same in the system. Additionally, for $\Pr < 1$, the thermal diffusivity is higher than the viscous diffusivity and hence thermal fraction has been reduced. The influence of the measure of the strength of the heterogeneous chemical reaction k_s on the mass fraction of the nanofluid is discussed in Fig. (12). It is observed that developing values of k_s reduces concentration boundary-layer thickness from *MgO*-H_2O nanofluid to *Cu*-H_2O nanofluid. That is a reduction of concentration during both the liquids occurs due to the presence of reactions in the system. Again, Fig. (13) is presented to show the influence of the measure of the strength of the homogeneous reaction (k) on the mass fraction of the nanofluid. Improving amount of k declines the concentration boundary-layer thickness of the present fluids, thereby the mass fraction of the system reduces during both the liquids.

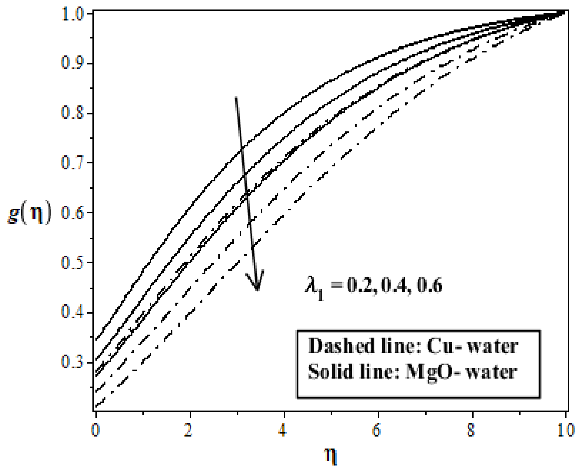

Figure 9. Action of λ_1 on mass fraction of the fluid.

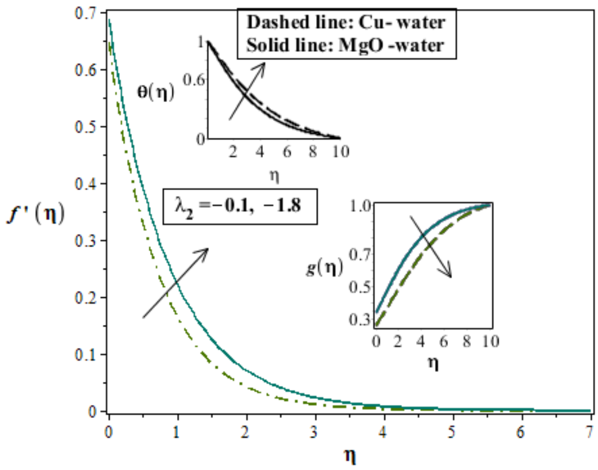

Figure 10. Action of λ_2 on the velocity, temperature and mass fraction pattern.

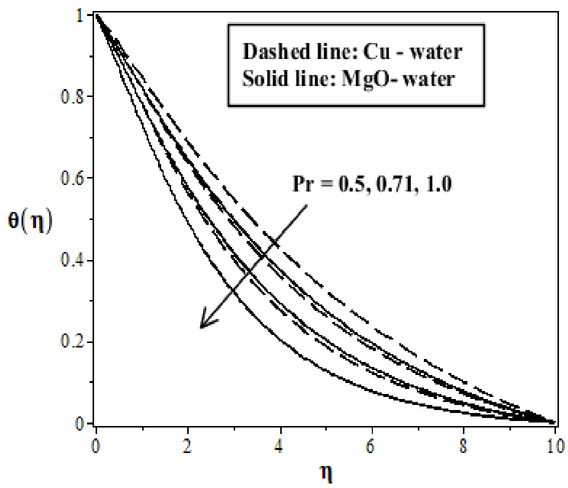

Figure 11. Action of Pr on the temperature distributions of the nanofluid.

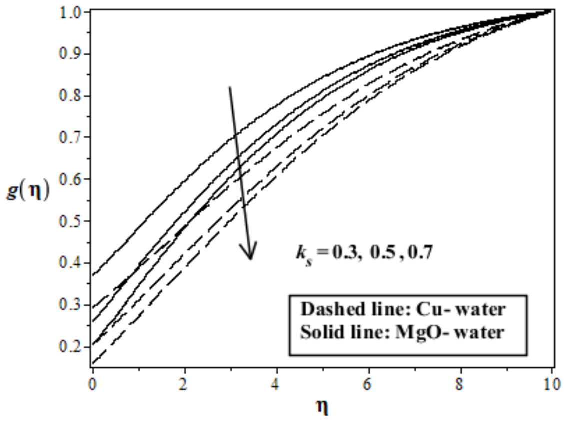

Figure 12. Action of k_s on the mass fraction of the nanofluid.

From Figs. (12) and (13), it is noticed that range of the concentration is more during the variation of homogeneous chemical reaction than the heterogeneous reaction.

Table 2 is submitted to validate our numerical codes with the previous results of Hayat *et al.* (2017) and Almutairi *et al.* (2019) in the absence of energy equation and second-order velocity slip condition. They have studied the effects of both homogeneous and heterogeneous chemical reactions on the nanofluid containing different nanoparticles. We have compared our numerical results of skin friction coefficient of *Cu-H*$_2$*O* with the results reported in Hayat *et al.* (2017) and Almutairi *et al.* (2019) and achieved good conformity

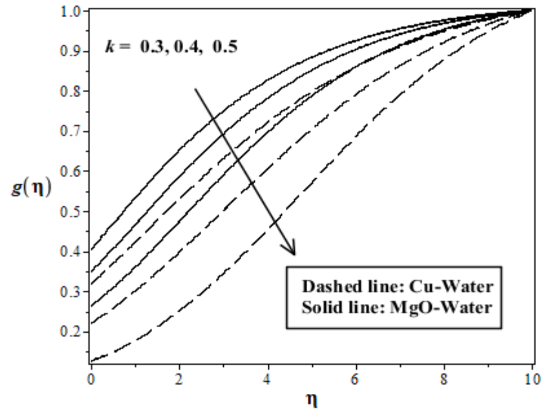

Figure 13. Action of k on the mass fraction of the nanofluid.

Table 2. Comparison of numerical values of skin friction coefficient of *Cu-H*$_2$*O* with the results of Hayat *et al.* (2017) and Almutairi *et al.* (2019).

ϕ	λ_1	M	k_s	Skin friction coefficient $(-f''(0))$ Hayat *et al.*	Almutairi *et al.*	Present Result
0.05				1.278	1.23278	1.2332778
0.1	1.0	0.5	0.3	1.465	1.41390	1.4138984
0.2				1.955	1.88407	1.8840684
	0.1			4.542	4.31610	4.3161033
0.2	0.5	0.5	0.3	2.827	2.70491	2.7049073
	0.9			2.079	2.00347	2.0034739
		0.1		1.897	1.81545	1.8154477
0.2	1.0	0.3	0.3	1.928	1.85097	1.8509724
		0.7		1.981	1.91500	1.9150037

Numerical values of physical quantities that are important in different physical fields are tabulated through some novel flow parameters in Table 3. The skin friction coefficient which helps us to measure the drag force of the fluid at the flow surface of *Cu-H*$_2$*O* nanofluid rises with ϕ, but an opposite nature is observed in the case of *MgO-H*$_2$*O* nanofluid. The heat transfer rate (Nusselt number) of the nanofluid at the surface decreases with the improving values of ϕ But, it enhances the mass accumulation rate (Sherwood number) during the nanofluid containing *Cu* nanoparticle and an opposite behaviour is noticed in the case of *MgO-H*$_2$*O* nanofluid. From this table, it is perceived that the magnetic parameter helps to control the heat transfer rate of the nanofluid. But it enhances the other two physical quantities during both the liquids. The physical quantities during both the liquids except skin friction coefficient increase with the effects of first-order velocity slip. That is the skin friction coefficient of the nanofluids drops down with the influence of 1st order velocity slip. From this table, it is also achieved that the combination of *MgO* and water generates more heat transfer rate at the surface than the *Cu* -water nanofluid. So, *MgO* -water nanofluid plays an important role to enhance the heat transfer rate.

Table 3. Numerical values of physical quantities for various values of flow parameters when $Pr = 7$, $Sc = 0.23$, $k_s = 0.5$, $Ec = 1$, $\lambda_2 = -1$.

ϕ	M	λ_1	Skin friction coefficient $[-f'(0)]$		Nusselt number $[-\theta'(0)]$		Sherwood number $[-g'(0)]$	
			Cu	MgO	Cu	MgO	Cu	MgO
0.05			3.003282	2.876463	0.370456	0.394243	-0.110886	-0.121756
0.1	0.5	0.3	3.055699	2.832283	0.294899	0.341023	-0.106331	-0.125451
0.2			3.083488	2.725534	0.195446	0.255932	-0.103915	-0.134106
	0.5		3.083488	2.725534	0.195446	0.255932	-0.103915	-0.134106
0.2	1.0	0.3	3.308428	2.907266	0.130745	0.200470	-0.084969	-0.119147
	1.5		3.499177	3.065679	0.081130	0.155603	-0.070914	-0.105463
		0.5	4.506724	3.770164	0.169504	0.255656	-0.123267	-0.142697
0.2	0.3	1.0	3.083488	2.725534	0.195446	0.255932	-0.095464	-0.121508
		1.5	2.208204	2.019088	0.198133	0.244226	-0.069878	-0.097835

VI. CONCLUSION

It is clearly noticed that all the figures satisfy the far-field boundary conditions asymptotically. The Maple-18 software is one of the most powerful math engines that helps us to calculate, visualize, explore and solve mathematical problems without any complexity. From this analysis, we have summarized the outcomes as follows:

i. With the help of applying a magnetic field, we can control the motion of the nanofluid, but we should keep in mind that an excessive amount of magnetic parameter may damage the system by burning and over deposition of mass. Also, it enhances the drag force and mass accumulation rate of the fluid during both the liquids at the surface of the sheet.

ii. The velocity pattern during both the liquids behaves like a decreasing function of the volume fraction of the particles. On the other hand, the thermal and mass fractions of the nanofluid characterize an increasing function of the volume fraction of the particles. Again, for better achievement of thermal transmission rate at the surface, the nanofluid containing *MgO* nanoparticle is more efficient than the nanofluid containg *Cu* nanoparticle. Also, this nanoparticle gives fewer effects of drag force and mass accumulation rate at the surface than *Cu*-H_2O nanofluid.

iii. Due to the effects of the second-order velocity slip parameter, the motion, as well as the temperature of the nanofluid accelerates, but an opposite nature is observed for the mass fraction of the fluid.

iv. The mass fraction of the nanofluid during both the nanoparticles reduces with the improving measures of both heterogeneous and homogeneous chemical reaction factors.

v. It is seen from the Table-3 that the combination of *MgO* and water generates less shear stress at the surface in comparison to *Cu*-water nanofluid. So, *MgO* and water is a better combination to use in industrial purpose because more shear stress may damage the system.

NOMENCLATURE

c,a_0 constants
A, B chemical species
a & b concentration of A & B, respectively (*mol/kg*).
$f'(\eta)$ dimensionless stream function
$g(\eta)$ dimensionless mass fraction
Ec Eckert number
K_n Knudsen number
Nu_x local Nusselt number
D_A & D_B mass diffusion for A & B (m^2/s)
k measure of the strength of the homogeneous reaction (s^{-1})
k_s measure of the strength of the heterogeneous chemical reaction (s^{-1})
M magnetic parameter
Pr Prandtl number
K porosity of the porous medium
K_c & K_s rate constants
B_0 strength of magnetic field (*Tesla*)
Sc Schmidt number
C_f skin friction coefficient
C_P specific heat at constant pressure (*J/kgK*)
T temperature of the fluid (*K*)
k thermal conductivity (*W/mK*)
u velocity component along x-direction (*m/s*)
v velocity component along y-direction (*m/s*)

Greek symbols:

ρ density (kg/m^3)
μ dynamic viscosity (*Pa s*)
$\theta(\eta)$ dimensionless stream function
σ electrical conductivity (*s/m*)
λ_1, λ_2 first and second order velocity slip parameter
υ kinematic viscosity (m^2/s)
δ_1 molecular mean free path (*m*)
ε momentum accommodation coefficient
λ porosity parameter
δ ratio of the diffusion coefficient
η similarity variable
ψ stream function
ϕ volume fraction of the particle

Subscripts:

w at wall
∞ at free stream region
nf nanofluid
f base fluid
s solid particle"

REFERENCES

Abbas, Z., Rafiq, M.Y., Hasnian, J. and Nadeem, A. (2021) Thermally developed generalized Bodewadt flow containing nanoparticles over a rotating surface with slip condition. *International*

Communications in Heat and Mass Transfer. 122, 105143.

Anuar, N.S., Bachok, N., Arifin, N.M. and Rosali, H. (2019) Effect of suction/injection on stagnation point flow of hybrid nanofluid over an exponentially shrinking sheet with stability analysis. *CFD Lett.* **11**, 21–33.

Alzahrani, A.K., Ullah, M.Z., Alshomrani, A.S. and Gul, T. (2021) Hybrid nanofluid flow in a Darcy-Forchheimer permeable medium over a flat plate due to solar radiation. *Case Stud. Therm. Eng.* **26**, 100955.

Almutairi, F., Khaled, S.M. and Ebaid, A. (2019) MHD flow of nanofluid with homogeneous-heterogeneous reactions in a porous medium under the influence of second-order velocity slip. *Mathematics.* **7**, 220.

Aziz, A. (2009) A similarity solution for laminar boundary layer over a flat plate with a convective surface boundary condition. *Commun Nonlinear Sci Number Simulat.* **14**, 1064-1068.

Bachok, N., Ishak, A. and Pop, I. (2013) Mixed Convection Boundary Layer Flow over a Moving Vertical Flat Plate in an External Fluid Flow with Viscous Dissipation Effect. *PloS ONE***. 8**, e60766.

Crane, L.J. (1970) Flow past a stretching plate. *Zeitschrift für Angew. Math. und Phys. ZAMP*. **21**, 645–647.

Choi, S. U. S. (1995) Enhancing thermal conductivity of uids with nanoparticles. *Proceedings of the 1995 ASME Int. Mech. Eng. Cong. and Exposition, San Francisco, USA, ASME FED 231/MD.* 99–105.

Chanie, A. G., Shankar, B. and Nandeppanavar, M. M. (2018) MHD flow of nanofluids through a porous media due to a permeable stretching sheet. *J. Nanofluids*. **7**, 488–498.

Dey, D. and Borah, R. (2020) Dual Solutions of Boundary Layer flow with Heat and Mass Transfers over an Exponentially Shrinking cylinder: Stability Analysis. *Lat. Am. Appl. Res.* **50**, 247–253.

Dey, D. and Borah, R. (2021) Stability analysis on dual solutions of second- grade fluid flow with heat and mass transfers over a stretching sheet. *Int. J. Thermofluid Sci. Technol.* **8**, 080203.

Dey, D., Borah, R. and Mahanta, B. (2021) Boundary Layer Flow and Its Dual Solutions Over a Stretching Cylinder: Stability Analysis. in *Emerging Technologies in Data Mining and Information Security. Advances in Intelligent Systems and Computing.* 27–38.

Dey, D., Hazarika, M. and Borah, R. (2021) Entropy generation analysis of magnetized micropolar fluid streaming above an exponentially extending plane. *Lat. Am. Appl. Res.* **51**, 255-260.

Dey, D., Borah, R. and Khound, A.S. (2022) Stability analysis on dual solutions of MHD Casson fluid flow with thermal and chemical reaction over a permeable elongating sheet. *Heat Transfer*. **51,** 3401-3417.

Dey, D. and Hazarika, M. (2021) Entropy Generation Analysis and Slip Effects on Nano Fluid Flow with Heat and Mass Transfer. *Advances in Thermofluids and Renewable Energy. Proceedings of TFRE 2020*. 59–71.

Dey, D. and Chutia, B. (2020) Dusty nanofluid flow with bioconvection past a vertical stretching surface. *J. King Saud Univ. - Eng. Sci*. **34**, 375-380.

Dey, D. and Hazarika, M. (2022) Entropy Generation Analysis of Al2O3-Water Nanofluid Flow Past a Permeable Cone Under the Effect of Suction/Injection and Viscous Ohmic Dissipations. *Journal of Engineering Physics and Thermophysics.* **95,** 961-969.

Doh, D. H., Muthtamilselvan, M., Swathene, B. and Ramya, E. (2020) Homogeneous and heterogeneous reactions in a nanofluid flow due to a rotating disk of variable thickness using HAM. *Math. Comput. Simul.* **168**, 90–110.

Fang, T.,Yao, S., Zhang, J. and Aziz, A. (2010) Viscous flow over a shrinking sheet with a second order slip flow model. *Commun. Nonlinear Sci. Numer. Simul.* **15**, 1831–1842.

Fang, T. and Aziz, A. (2010) Viscous flow with second-order slip velocity over a stretching sheet. *Zeitschrift fur Naturforsch. - Sect. A J. Phys. Sci.* **65**, 1087–1092.

Hasnain, J. and Abid, N. (2022) Numerical investigation for thermal growth in water and engine oil-based ternary nanofluid using three different shaped nanoparticles over a linear and nonlinear stretching sheet. *Numerical Heat Transfer, Part A: Applications.* In print.

Hasnain, J., Satti, H.G., Sheikh, M. and Abbas, Z. (2022) *Study of double slip boundary condition on the oscillatory flow of dusty ferrofluid confined on a permeable channel.* FACTA UNVERSITATIS Series: Mechanical Engineering.

Hasnain, J., Sheikh, M. and Abbas, Z. (2021) Navier slip and suction/injection effects on ascillatory flow of nanofluid with fluid-particle interection in a channel. *E3S Web of Conference.* **321**, 04002.

Hasnain, J. and Abbas, Z. (2019) Entropy generation analysis on two phase Micropolar Nanofluids flow in an inclined channel with convective heat transfer. *Thermal Science.* **23**, 1765-1777.

Hussain, S.T., Nadeem, S. and Haq, R. U. (2014) Model-based analysis of micropolar nanofluid flow over a stretching surface. *Eur. Phys. J. Plus*. **129**, 161.

Hayat, T., Imtiaz, M., Alsaedi, A. (2017) Magnetohydrodynamic flow of nanofluid with homogeneous-heterogeneous reactions and velocity slip. *Therm. Sci.* **21**, 901–913.

Ho, C. J., Cheng, C. Y., Yang, T. F., Rashidi, S. and Yan,

W. M. (2021) Cooling characteristics and entropy production of nanofluid flowing through tube. *Alexandria Eng. J*. **61**, 427-441.
Ismail, H.N., Megahed, A.A., Abdel-Wahed, M.S. and Omama, M. (2018) Thermal radiative effects on MHD casson nanofluid boundary layer over a moving surface. *J. Nanofluids*. **7,** 910–916.
Jeevandhar, S.P., Kedla, V., Gullapalli, N. and Thavada, S.K. (2021) Natural Convective Effects on MHD Boundary Layer Nanofluid Flow over an Exponentially Accelerating Vertical Plate. *Biointerface Research in Applied Chemistry*. **11**, 13790-13805.
Jamshed, W., Devi S, S.U., Goodarzi, M., Prakash, M., Nisar, K.S., Zakarya, M. and Abdel-Aty, A.H. (2021) Evaluating the unsteady Casson nanofluid over a stretching sheet with solar thermal radiation: An optimal case study. *Case Stud. Therm. Eng.* **26**, 101160.
Khashi'ie, N.S., Arifin, N.M., Rashidi, M.M., Hafidzuddin, E.H. and Wahi, N. (2019) Magnetohydrodynamics (MHD) stagnation point flow past a shrinking/stretching surface with double stratification effect in a porous medium. *J. Therm. Anal. Calorim.* **139**, 3635–3648.
Markin, J.H. (1996) A Model for Isothermal Homogeneous-Heterogeneous Reactions in Boundary Layer Flow. *Math. Comput. Model.* **24**, 125–136.
Malik, R. and Khan, M. (2018) Numerical study of homogeneous–heterogeneous reactions in Sisko fluid flow past a stretching cylinder. *Results Phys.* **8**, 64–70.
Mehdi, I., Abbas, Z. and Hasnain, J. (2022) MHD flow and heat transfer between two rotating disks under the effects of nanomaterials (MoS_2) and thermal radiation. *Case Studies in Thermal Engineering.* **33**, 101968.
Mishra, A., Pandey, A.K. and Kumar, M. (2019) Velocity, thermal and concentration slip effects on MHD silver-water nanofluid flow past a permeable cone with suction/injection and viscous-ohmic dissipation. *Heat Transf. Res.* **50**, 1351–1367.
Muhammad, S., Khan, H., Ali, G., Ali Shah, S.I., Ishaq, M. and Hussain, S.A. (2019) Stagnation point nanofluid flow of Cu and Ag nanoparticles over a stretching surface with magnetic effects. *J. Nanofluids.* **8**, 1314–1318.
Naveed, M., Ali, S., Hasnain, J. and Abbas, Z. (2021) Analysis of the effect of Joule heating and Hall current on flow of Hybrid Nanofluid over a Curved Stretching surface with Melting Boundary condition. *Heat Transfer Research.* **52**, 1-16.
Prasannakumara, B.C. (2021) Numerical simulation of heat transport in Maxwell nanofluid flow over a stretching sheet considering magnetic dipole effect. *Partial Differ. Equations Appl. Math.* **4**, 100064.
Rahman, M.M. and Eltayeb, I.A. (2013) Radiative heat transfer in a hydromagnetic nanofluid past a non-linear stretching surface with convective boundary condition. *Meccanica*. **48**, 601-615.
Rajesh, V., Srilatha, M. and Chamkha, A.J. (2020) Hydromagnetic effects on hybrid nanofluid (Cu–al2O3/Water) flow with convective heat transfer due to a stretching sheet. *J. Nanofluids.* **9**, 293–301.
Shravani, I., Ramya, D. and Joga, S. (2018) Heat and mass transfer in stagnation point flow over a stretching sheet with chemical reaction and suction/injection in nanofluids. *J. Nanofluids*. **7**, 862–869.
Sheikh, M., Abbas, Z., Hasnain, J., Nadeem, A. and Sajid, M. (2021) Impact of nonlinear Rosseland Approximation on flow of Newtonian fluid with Unequal diffusivities of chemically reactive species. *Arabian Journal for Science and Engineering.* **46**, 2711-2719.
Sheikh, M. and Abbas, Z. (2017) Homogeneous–heterogeneous reactions in stagnation point flow of Casson fluid due to a stretching/shrinking sheet with uniform suction and slip effects. *Ain Shams Eng. J.* **8**, 467–474.
Waini, I., Ishak, A. and Pop, I. (2021) Hybrid nanofluid flow with homogeneous-heterogeneous reactions. *Comput. Mater. Contin.* **68**, 3255–3269.
Zehra, I., Abbas, N., Amjad, M., Nadeem, S., Saleem, S. and Issakhov, A. (2021) Casson nanoliquid flow with Cattaneo-Christov flux analysis over a curved stretching/shrinking channel. *Case Stud. Therm. Eng.* **27**, 101146.

Received: March 29, 2022
Sent to Subject Editor: May 12, 2022
Accepted: September 14, 2022
Recommended by Subject Editor Fabio Giannetti